Low-Temperature Solution-Mediated Synthesis of Polycrystalline Intermetallic Compounds from Bulk Metal Powders

Nathaniel L. Henderson and Raymond E. Schaak*

Department of Chemistry, The Pennsylvania State University, University Park, Pennsylvania 16802

Received January 24, 2008. Revised Manuscript Received February 28, 2008

A variety of binary intermetallic compounds of late transition metals with low-melting post-transition metals have been synthesized in bulk quantities by reacting molten metal dispersions with fine metal powders in hot polyalcohol solvents. Fourteen distinct intermetallics were formed using this technique: SbSn, $FeSn_2$, Cu_6Sn_5, $CoSn_3$, Ni_3Sn_4, $FeGa_3$, $NiGa_4$, Cu_9Ga_4, $CoGa_3$, Ni_2In_3, InSb, In_5Bi_3, InBi, and Bi_3Ni. Notable among these are a low-temperature phase (α-$CoSn_3$), textured intermetallic powders with anisotropic morphologies (α-$CoSn_3$ and $FeSn_2$), and superconductors (Bi_3Ni and In_5Bi_3). Reaction pathway studies suggest that the molten low-melting metals diffuse into the larger higher melting powders, forming intermetallic compounds directly in a liquid-phase medium from bulk-scale powders of the constituent elements.

Introduction

Intermetallic compounds comprise a large family of crystalline solids that generally contain two or more metallic elements and have crystal structures that differ from those of their constituent elements. These materials are widely used in technological applications because of their important physical properties, which include superconductivity,[1,2] shape memory effects,[3,4] permanent magnetism,[5] catalytic activity,[6] and lithium and hydrogen storage capacity.[7] Traditionally, intermetallics are synthesized using high-temperature methods such as arc melting, powder metallurgy, and induction heating. Such reaction conditions, combined with long annealing times and frequent regrinding steps for powder preparations, are necessary to overcome the limitations of solid–solid diffusion.

Alternative strategies that yield intermetallics at lower temperatures are becoming increasingly common. For example, work by Johnson and co-workers has shown that new and metastable antimonides, including $FeSb_3$, $NiSb_3$, and $RuSb_3$, can be accessed at low annealing temperatures (<500 °C) through controlled diffusion of layered, elementally modulated precursors.[8] Additional low-temperature approaches include molten flux synthesis,[9] solvothermal techniques,[10] electrodeposition,[11] high-energy ball milling,[12] chemical vapor deposition (CVD),[13] and gas-phase condensation routes.[14] Solution-mediated routes have also proven to be viable strategies for low-temperature synthesis, yielding many known intermetallics as well as several new and metastable phases.[15,16] There are many reasons for develop-

* To whom correspondence should be addressed. E-mail: schaak@chem.psu.edu.

(1) (a) Nagamatsu, J.; Nakagawa, N.; Muranaka, T.; Zenitani, Y.; Akimitsu, J. *Nature* **2001**, *410*, 63. (b) Cava, R. J.; Takagi, H.; Batlogg, B.; Zandbergen, H. W.; Krajewski, J. J.; Peck, W. F.; Vandover, R. B.; Felder, R. J.; Siegrist, T.; Mizuhashi, K.; Lee, J. O.; Eisaki, H.; Carter, S. A.; Uchida, S. *Nature* **1994**, *367*, 146.

(2) Kunzler, J. E.; Buehler, E.; Hsu, F. S. L.; Wernick, J. H. *Phys. Rev. Lett.* **1961**, *6*, 89.

(3) (a) Cui, J.; Shield, T. W.; James, R. D. *Acta Mater.* **2004**, *52*, 35. (b) Stern, R. A.; Willoughby, S. D.; MacLaren, J. M.; Cui, J.; Pan, Q.; James, R. D. *J. Appl. Phys.* **2003**, *93*, 8644–8646.

(4) Takeuchi, I.; Famodu, O. O.; Read, J. C.; Aronova, M. A.; Chang, K.-S.; Craciunescu, C.; Lofland, S. E.; Wuttig, M.; Wellstood, F. C.; Knauss, L.; Orozco, A. *Nat. Mater.* **2003**, *2*, 180.

(5) (a) Sun, S.; Murray, C. B.; Weller, D.; Folks, L.; Moser, A. *Science* **2000**, *287*, 1989–1992. (b) Paduani, C. *J. Appl. Phys.* **2001**, *90*, 6251.

(6) Casado-Rivera, E.; Volpe, D. J.; Alden, L.; Lind, C.; Downie, C.; Vazquez-Alvarez, T.; Angelo, A. C. D.; DiSalvo, F. J.; Abruna, H. D. *J. Am. Chem. Soc.* **2004**, *126*, 4043.

(7) (a) Rönnebro, E.; Yin, J.; Kitano, A.; Wada, M.; Sakai, T *Solid State Ionics* **2005**, *176*, 2749. (b) Shi, L.; Li, H.; Wang, Z.; Huang, X.; Chen, L. *J. Mater. Chem.* **2001**, *11*, 1502. (c) Mukaibo, H.; Osaka, T.; Reale, P.; Panero, S.; Scrosati, B.; Wachtler, M. *J. Power Sources* **2003**, *132*, 225. (d) Kirchheim, R.; Mutschele, T.; Keininger, W.; Gleiter, H.; Birringer, R.; Koble, T. D. *Mater. Sci. Eng.* **1988**, *99*, 457–462.

(8) (a) Jensen, J. M.; Ly, S.; Johnson, D. C. *Chem. Mater.* **2003**, *15*, 4200. (b) Smalley, A. L. E.; Kim, S.; Johnson, D. C. *Chem. Mater.* **2003**, *15*, 3847. (c) Smalley, A. L. E.; Jespersen, M. L.; Johnson, D. C. *Inorg. Chem.* **2004**, *43*, 2486.

(9) (a) Kanatzidis, M. G.; Pottgen, R.; Jeitschko, W. *Angew. Chem., Int. Ed.* **2005**, *44*, 6996. (b) Fisk, Z.; Remeika, J. P. *Handbook on the Physics and Chemistry of Rare Earths*; 1989; Vol. 12, p 55.

(10) Heibel, M.; Kumar, G.; Wyse, C.; Bukovec, P.; Bocarsly, A. B. *Chem. Mater.* **1996**, *8*, 1504.

(11) Martin-Gonzalez, M.; Prieto, A. L.; Knox, M. S.; Gronsky, R.; Sands, T.; Stacy, A. M. *Chem. Mater.* **2003**, *15*, 1676.

(12) (a) Koch, C. C.; Whittenberger, J. D. *Intermetallics* **1996**, *4*, 339–355. (b) Meitl, M. A.; Dellinger, T. M.; Braun, P. V. *Adv. Funct. Mater.* **2003**, *13*, 795. (c) Konrad, H.; Weissmuller, J.; Birringer, R.; Karmonik, C.; Gleiter, H. *Phys. Rev. B* **1998**, *58*, 2142.

(13) (a) Onda, A.; Komatsu, T.; Yashima, T. *J. Catal.* **2001**, *201*, 13–21. (b) Komatsu, T.; Inaba, K.; Uezono, T.; Onda, A.; Yashima, T. *Appl. Catal., A* **2003**, *251*, 315–326. (c) Mathur, S.; Veith, M.; Ruegamer, T.; Hemmer, E.; Shen, H. *Chem. Mater.* **2004**, *16*, 1304.

(14) Sanchez-Lopez, J. C.; Gonzalez-Elipe, A. R.; Fernandez, A. *J. Mater. Res.* **1998**, *13*, 703.

(15) (a) Leonard, B. M.; Bhuvanesh, N. S. P.; Schaak, R. E. *J. Am. Chem. Soc.* **2005**, *127*, 7326. (b) Dinega, D.; Bawendi, M. G. *Angew. Chem., Int. Ed.* **1999**, *38*, 1788.

(16) (a) Schaak, R. E.; Sra, A. K.; Leonard, B. M.; Cable, R. E.; Bauer, J. C.; Han, Y.-F.; Means, J.; Teizer, W.; Vasquez, Y.; Funck, E. S. *J. Am. Chem. Soc.* **2005**, *127*, 3506. (b) Cushing, B. L.; Kolesnichenko, V. L.; O'Connor, C. J. *Chem. Rev.* **2004**, *104*, 3893. (c) Masala, O.; Seshadri, R. *Annu. Rev. Mater. Res.* **2004**, *34*, 41. (d) Ung, D.; Soumare, Y.; Chakroune, N.; Viau, G.; Vaulay, M.-J.; Richard, V.; Rievet, F. *Chem. Mater.* **2007**, *19*, 2084.

10.1021/cm800245j CCC: $40.75
Published on Web 04/22/2008

Table 1. Synthetic Conditions for Binary Intermetallics[a]

intermetallic phase	reaction temp. (°C)	time at reaction temp. (h)
SbSn	280	12.0
$FeSn_2$	260	5.0
Cu_6Sn_5	280	2.5
α-$CoSn_3$	260	2.5
Ni_3Sn_4	270	4.0
$FeGa_3$	270	12.0
$NiGa_4$	260	3.0
Cu_9Ga_4	280	18.0
$CoGa_3$	250	18.0
Ni_2In_3	260	3.0
InSb	290	6.0
In_5Bi_3	80	16.0
InBi	105	16.0
Bi_3Ni	260	4.0

[a] All intermetallics were synthesized in TEG except InBi and In_5Bi_3, which were synthesized in DEG.

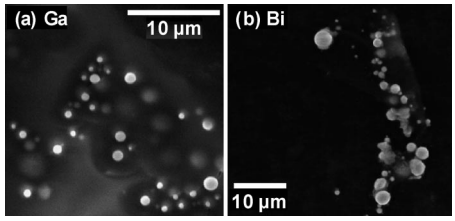

Figure 1. SEM images of PVP-stabilized (a) Ga and (b) Bi colloids obtained by dispersing Ga shot and Bi powder in hot tetraethylene glycol and rapidly quenching in ethanol.

ing and utilizing these lower temperature methods for the synthesis of intermetallic compounds. In addition to facilitating exploratory synthesis and stabilizing low-temperature phases, these synthetic routes provide different processing capabilities and sometimes allow kinetic control over phase formation. This is often accomplished by minimizing diffusion lengths and increasing reactivity. By overcoming the rate-limiting diffusion step, these methods can access materials unattainable through traditional high-temperature synthetic methods.

Here, we describe a new strategy for synthesizing bulk-scale microcrystalline powders of intermetallic compounds using "beaker chemistry" reactions. This approach bridges the gap between molten metal flux techniques[9] that yield bulk crystals of intermetallic compounds and solution chemistry techniques that yield metal and intermetallic nanocrystals.[15,16] Dispersions of molten metals are prepared by heating low-melting metals (Ga, Sn, In, and Bi) in high-boiling polyalcohol (polyol) solvents with vigorous stirring, in direct analogy to the method used by Xia and co-workers to obtain single-metal colloids (Bi and In).[17] In addition to providing a heat source, the solvent helps to maintain a reducing atmosphere. These dispersions are reacted with bulk powders of late-transition metals and *p*-block metals under flowing argon and annealed in solution to yield the final intermetallic phase. This method has proven to be general for a wide range of binary phases and provides facile access to low-temperature structures (α-$CoSn_3$), superconducting phases (In_5Bi_3, Bi_3Ni), and textured or highly anisotropic intermetallics ($FeSn_2$, α-$CoSn_3$). Polycrystalline samples can be rapidly obtained in bulk form, potentially providing a pathway for rapid exploratory synthesis of intermetallics and alloys in an underexplored, low-temperature regime.

(17) Wang, Y.; Xia, Y. *Nano Lett.* **2004**, *4*, 2047.

Experimental Section

Materials. The following chemicals were used as purchased without further purification: Co (99.8%), Cu (99%), Sn (99.8%), In (99.99%), Sb (99.5%), Ni (99.8%), and Bi (99.5%) powders (−325 mesh, Alfa Aesar); Fe powders (−325 mesh, 99%, Alfa Aesar; 1–3 μm, 98%, Alfa Aesar); Ga shot (6 mm shot broken into ∼1 mm pieces, 99.9999%, Alfa Aesar), tetraethylene glycol (TEG, 99%, Alfa Aesar), diethylene glycol (DEG, 99%, Alfa Aesar), and poly(vinyl pyrrolidone) (PVP; MW = 40 000, Alfa Aesar).

Synthesis. In a typical, one-pot synthesis, stoichiometric amounts of the two constituent metals (approximate total mass of 0.15 g) are added to a flask with 30 mL of TEG (bp = 314 °C) or DEG (bp = 245 °C) depending on the desired maximum attainable temperature. After purging the system with Ar, the solution is rapidly heated (∼5–10 °C/min) with continuous stirring (500–1000 rpm) and then maintained at the peak temperature until the reaction is complete. No polymers or additional surfactants are used in the synthesis, unless otherwise noted.

The relevant synthetic details for each system are given in Table 1. Powders of intermetallics are obtainable at temperatures ranging from 85 to 300 °C, and complete reaction can require as few as 3 h or as many as 18 h at the peak temperature. Typically, formation of intermetallics is detectable by powder X-ray diffraction (XRD) in 1–3 h. A slight excess of the low-melting metal remains unreacted when magnetic elements are used (Fe, Co, Ni) due to magnetic attraction to the stir bar, which affects the available stoichiometry. The excess low-melting metal is easily removed by briefly sonicating in ∼2 M HCl.

Larger (∼50 μm) rod-shaped crystals of $FeSn_2$ were grown by adding a 2-fold excess of Sn powder to the initial solution, discontinuing stirring after formation of the intermetallic phase, and annealing in the hot solvent (260 °C) for 48 h under flowing Ar. Fe powders (1–2 μm) were used for the crystal growth to facilitate rapid Sn diffusion. $FeSn_2$ rods were collected from the obtained shot by dissolving the excess Sn matrix in dilute HCl for 1 h.

Characterization. Powder XRD data were collected using a Bruker-AXS D8 Advance Diffractometer with a scintillation counter and a Bruker D8 Advance Diffractometer with a LynxEye 1D-detector (both using Cu Kα radiation). XRD patterns were obtained from powdered samples at room temperature. Scanning electron microscopy (SEM), energy-dispersive X-ray spectroscopy (EDS), and elemental mapping data were collected using a JEOL JSM 5400 SEM operating at 20 kV. Magnetic characterization of superconducting phases was performed using a Quantum Design SQUID magnetometer.

Results and Discussion

Synthesis of Polycrystalline Intermetallics. Fourteen distinct binary intermetallic compounds were synthesized by reacting molten metal dispersions with fine metal powders in hot polyalcohol solvents. The synthesis approach requires that the molten metals melt below the solvent reflux temperature. This criterion is met by Sn (231.9 °C), Ga (29.8 °C), In (156.6 °C), and Bi (271.4 °C). In order to provide evidence for the formation of molten metal dispersions, Bi and Ga colloids were prepared by heating the elemental powders above their respective melting temperatures with vigorous stirring in TEG, mimicking the conditions of a

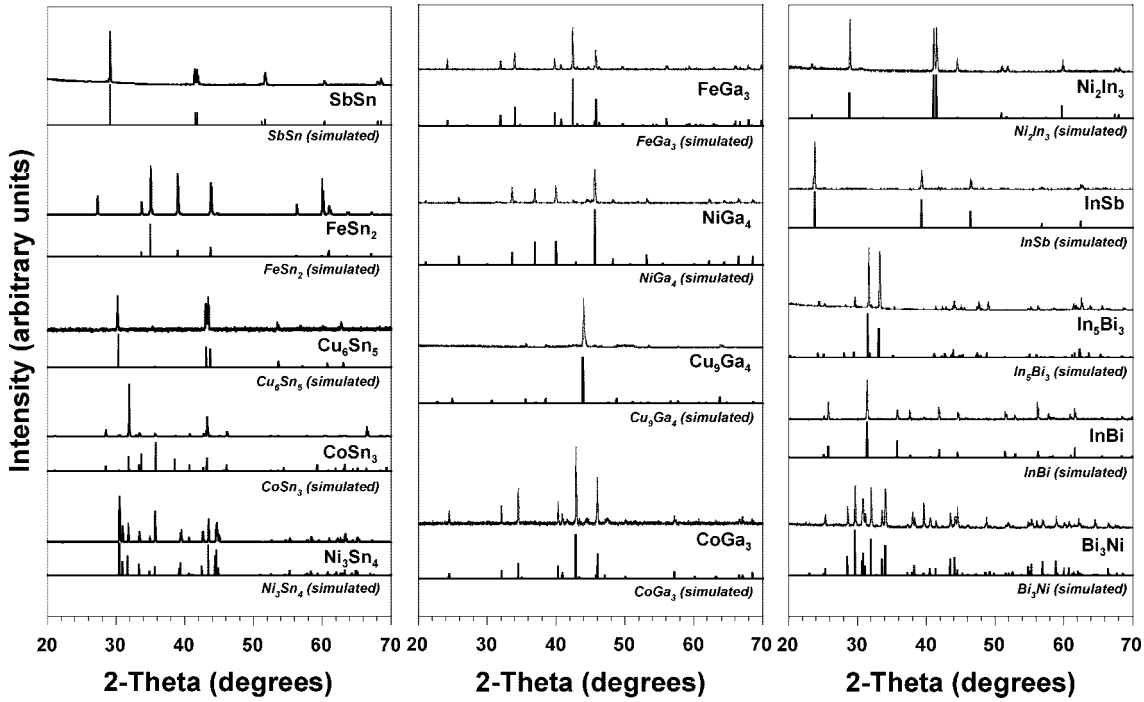

Figure 2. Powder XRD patterns of *M*−Sn, *M*−Ga, *M*−In, and *M*−Bi intermetallics formed by reacting molten metal dispersions in TEG with transition metal and p-block metal powders. Corresponding simulated patterns are shown below each observed pattern. With the exception of SbSn, all simulated patterns were calculated from crystallographic data. The simulated diffraction pattern for SbSn was taken from the JCPDS database (33-0118).

typical synthesis. These single-metal dispersions, similar to those obtained by Xia and co-workers,[17] were stabilized with poly(vinyl pyrrolidone) (PVP; MW = 40 000) and quenched in ethanol. As shown in Figure 1, the single-metal dispersions are comprised of small spherical droplets (<3 μm), which are much smaller in size than the starting materials (<45 μm for Bi, ~1 mm for Ga), and provide indirect evidence that the metal is molten and suspended in the hot polyol solvent.

Binary intermetallic phases are obtained when the molten dispersions are formed in the presence of transition metal and *p*-block metal powders. Figure 2 shows XRD data for fourteen *M*−Sn, *M*−Ga, *M*−In, and *M*−Bi intermetallic compounds that were synthesized using this strategy—SbSn, $FeSn_2$, Cu_6Sn_5, $CoSn_3$, Ni_3Sn_4, $FeGa_3$, $NiGa_4$, Cu_9Ga_4, $CoGa_3$, Ni_2In_3, InSb, In_5Bi_3, InBi, and Bi_3Ni. A few of these are highlighted in more detail below. Most compounds are phase pure within the detection limits of our laboratory X-ray diffractometer. However, diffraction patterns for $NiGa_4$ and InBi display small impurity peaks (~5%) attributable to other binary phases. Additionally, SbSn possesses a slight (~5%) excess of Sb, though this is consistent with known variations in stoichiometry for β-SbSn.[18] Representative SEM micrographs of $NiGa_4$, $FeGa_3$, and Ni_3Sn_4 are shown in Figure 3 along with element mapping data for Ni_3Sn_4 to confirm the composition (42% Ni, 58% Sn) and uniform elemental distribution. The crystallite sizes are generally between 5 and 30 μm, though this can vary for each system and with different annealing times. By altering the synthetic conditions, it is possible to obtain polycrystalline intermetallics

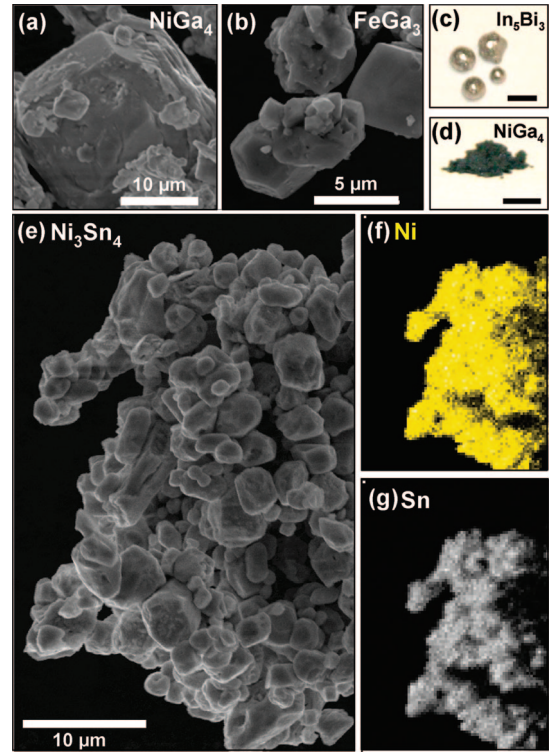

Figure 3. Representative SEM images of (a) $NiGa_4$, (b) $FeGa_3$, and (e) Ni_3Sn_4 powders. Elemental mapping data for (f) Ni and (g) Sn, along with EDS analysis, verify the composition of Ni_3Sn_4. Digital photographs of bulk-scale amounts of intermetallics obtainable through this synthetic method: (c) millimeter-scale shot (In_5Bi_3) and (d) bulk powder ($NiGa_4$). Scale bars in c and d are both 2 mm.

as both fused millimeter-sized shots (Figure 3c) and bulk-scale powders (Figure 3d). Though typical synthesis involves a one-step addition of both elemental precursors, intermetallic

(18) Noren, L.; Withers, R. L.; Schmid, S.; Brink, F. J.; Ting, V. *J. Solid State Chem.* **2006**, *179*, 404.

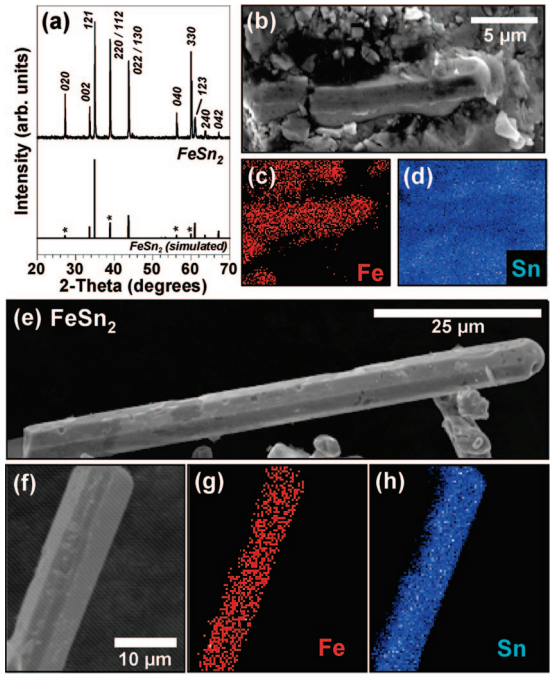

Figure 4. (a) Comparison between simulated and observed powder XRD patterns for crystalline $FeSn_2$ rods, highlighting the enhanced intensity for the *020*, *112/220*, *330*, and *040* reflections, indicated by asterisks in the simulated pattern. SEM imaging and elemental mapping (b−d) show that, following synthesis, $FeSn_2$ rods with octagonal cross-sections are embedded in a matrix of Sn metal. As shown in c and d, Fe is found mostly in rod-shaped crystals and Sn is everywhere. Following chemical removal of the excess Sn matrix, additional microscopy work confirms that the $FeSn_2$ rods are highly anisotropic (e,f). Elemental mapping of a single rod (f) shows that the particle is composed entirely of Fe (g) and Sn (h) in a 1:2 ratio.

formation was also observed when the transition metal and higher melting *p*-block metal powders were added to preformed dispersions of molten metal.

The $FeSn_2$ system provides an instructive example of the synthetic process and nature of the products that form. Upon inspection of the XRD data for $FeSn_2$ in Figure 2, it is evident that the intensities of the experimental data do not match those of the simulated XRD pattern. Figure 4a shows these XRD data in more detail along with several SEM micrographs (Figure 4b,e,f). In the observed diffraction pattern, the *020, 112/220*, *330*, and *040* reflections are noticeably more intense than the corresponding reflections in the simulated pattern. Though slight preferred orientation effects are not uncommon in the synthesis of intermetallics,[19] the large disparity of diffraction intensity suggests the presence of a significant amount of morphological anisotropy. Figure 4b shows a SEM micrograph of the $FeSn_2$ product synthesized with a 2-fold excess of Sn (in order to facilitate growth of larger crystallites). Element mapping data for this sample, shown in Figure 4c (Fe) and 4d (Sn), indicate that the Fe is localized in rod-like crystallites, while the Sn is present everywhere. The typical reaction workup involves dissolving the excess Sn with dilute HCl, leaving behind $FeSn_2$ without

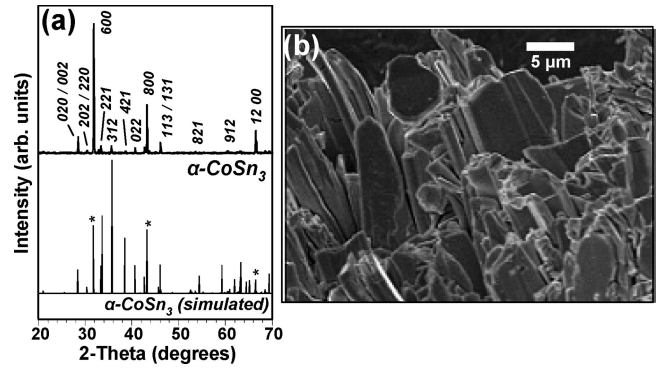

Figure 5. (a) Comparison between simulated and observed powder XRD patterns for $CoSn_3$. The *600*, *800*, and *12 00* reflections, indicated by asterisks, are much more intense than the corresponding peaks in the simulated pattern, suggesting preferred orientation parallel to [100]. This is supported by SEM imaging (b), which shows the plate-like morphology of the $CoSn_3$ particles.

Sn impurities. Accordingly, Figure 4e shows a SEM micrograph of the $FeSn_2$ product after dissolving the Sn matrix. Element mapping and EDS data for another rod (Figure 4f−h) confirm the 1:2 Fe:Sn ratio. As anticipated from the data in Figure 4a, the $FeSn_2$ crystallites are anisotropic and predominantly rod shaped. The $FeSn_2$ rods are observed to have an octagonal cross-section, which correlates well with growth along the [001] direction. The XRD data are consistent with this assignment, showing enhanced diffraction intensity for the {*hk*0} and {0*k*0} families of planes that would preferentially be parallel to the incident beam when the rods are oriented along their [001] growth direction.

Returning to the XRD data in Figure 2, preferred orientation is significant for $FeSn_2$ and α-$CoSn_3$ and to a lesser extent Ni_3Sn_4. $CoSn_3$ is a recently discovered layered intermetallic compound with two known polymorphs (α-$CoSn_3$ and β-$CoSn_3$), which differ primarily in stacking order.[20] $CoSn_3$ has been prepared using a lengthy peritectic reaction of $CoSn_2$ and excess Sn as well as through a Sn flux method.[20] Previously, we observed formation of nanocrystalline α-$CoSn_3$ by reacting β-Sn nanocrystals with $CoCl_2 \cdot 6H_2O$ in TEG at 180–195 °C under reducing conditions.[21] Here, we observe formation of bulk quantities of α-$CoSn_3$ at 260 °C in less than 3 h. Figure 5a compares the observed and simulated powder XRD patterns for α-$CoSn_3$, which show enhanced intensities corresponding to the {*h*00} family of planes. The SEM micrograph of α-$CoSn_3$ powder, shown in Figure 5b, confirms the platelet morphology of the crystallites and is consistent with the crystal structure of α-$CoSn_3$ and preferred orientation parallel to [100]. The XRD and SEM data clearly indicate that this synthetic method can produce textured microcrystalline powders of intermetallic compounds. Furthermore, the facile formation of α-$CoSn_3$ shows that low-temperature phases can be readily accessed using this synthetic method. For Ni_3Sn_4, the *200* reflection is more intense than the corresponding peak in the simulated diffraction pattern, suggesting some preferred orientation as well.

(19) (a) Suh, J. O.; Tu, K. N.; Tamura, N. *J. Appl. Phys.* **2007**, *102*, 063511. (b) Chen, C.; Ho, C. E.; Lin, A. H.; Luo, G. L.; Kao, C. R. *J. Electron Mater.* **2000**, *29*, 1200. (c) Stout, J. J.; Crimp, M. A. *Mater. Sci. Eng. A* **1992**, *152*, 335.

(20) Lang, A.; Jeitschko, W. *Z. Metallkd.* **1996**, *87*, 759.
(21) Chou, N. H.; Schaak, R. E. *J. Am. Chem. Soc.* **2007**, *129*, 7339.

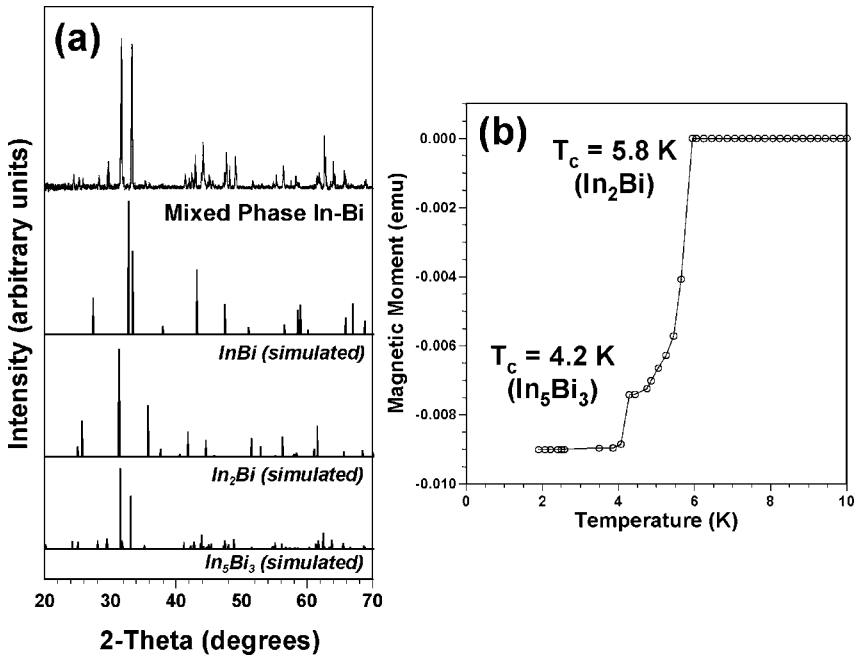

Figure 6. (a) Comparison between the observed powder XRD pattern for mixed-phase In−Bi and simulated patterns for InBi, In_2Bi, and In_5Bi_3. (b) Plots of magnetic moment vs temperature show superconducting transitions at 5.8 and 4.2 K, which are attributable to In_2Bi and In_5Bi_3, respectively.

Closer examination of the InBi and In_5Bi_3 diffraction patterns reveals impurities of In_2Bi, which is a known superconductor.[22] (Unfortunately, attempts to isolate phase-pure In_2Bi by increasing the amount of In have failed.) In_5Bi_3 is also a known superconducting phase.[23] Figure 6a shows powder XRD data for a representative sample of In-rich In−Bi, which includes InBi, In_2Bi, and In_5Bi_3. Figure 6b shows a plot of magnetic moment vs temperature for this mixed-phase In−Bi sample. The drop in magnetic moment at 5.8 K is consistent with the superconductor In_2Bi (T_c = 5.8 K). Likewise, the further drop at 4.2 K is consistent with the superconductor In_5Bi_3 (T_c = 4.2 K). InBi is not a known superconductor and does not contribute to the observed features in the low-temperature susceptibility data. Bi_3Ni is also a known superconductor (T_c = 4.06 K)[24] and readily accessible through this synthetic process. Figure 7 shows a plot of magnetic moment vs temperature for Bi_3Ni, showing a single superconducting transition near 4.0 K, which is consistent with that expected for Bi_3Ni. Importantly, observation of superconductivity in these samples, as-prepared and without additional annealing, shows that this synthetic method is viable for producing superconducting intermetallics.

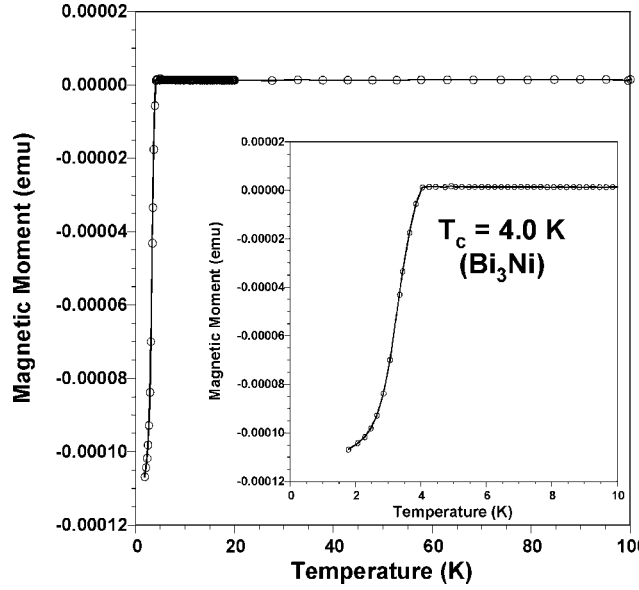

Figure 7. Plot of magnetic moment vs temperature for Bi_3Ni powder obtained by reacting Ni powder with dispersed molten Bi, showing a superconducting transition at 4.0 K, which is attributable to Bi_3Ni.

Investigation of the Reaction Pathway. Given the experimental details, there are two primary reaction pathways that could be involved in formation of intermetallics using this beaker-chemistry method. One possibility, in analogy to standard metal flux reactions, is that the molten metal droplets dispersed in the polyol solvent dissolve the other higher melting metal powders and subsequently precipitate the intermetallic powders. Another possibility is that the small droplets of molten metal attack the higher melting metal powders and form intermetallics via a diffusion-based process. Several control experiments imply that the latter pathway is more likely.

SEM images were obtained for the Ni precursor (Figure 8a) and Ni_2In_3 powder (Figure 8b) synthesized by reacting the Ni powder in a TEG dispersion of molten In. Prior to the reaction, the Ni grains are coarse, generally 10–20 μm in diameter, and possess sharp protrusions. After the reaction, the Ni_2In_3 grains remain similar in size and overall morphology to the Ni powder precursor, although the rough edges appear more smooth and contoured. The size retention and

(22) Schirber, J. E.; Van Dyke, J. P. *Phys. Rev. B* **1977**, *15*, 890.
(23) Canegallo, S.; Bicelli, L. P.; Serravalle, B.; Demeneopoulos, V. *J. Alloys Compd.* **1994**, *216*, 149.
(24) Jayaram, B.; Ekbote, S. N.; Narlikar, A. V. *Phys. Rev. B* **1987**, *36*, 1996.

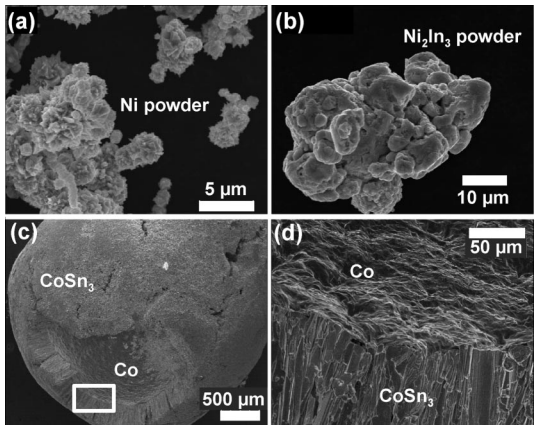

Figure 8. SEM images of the Ni powder (a) before and (b) after reaction with dispersed molten In. The general size and shape retention suggest that In diffuses into the surface of the Ni particles. (c,d) SEM images of $CoSn_3$ formed by reacting molten dispersed Sn with Co shot (~5 mm diameter). The central core of Co remains unreacted, while the surface forms $CoSn_3$ through Sn diffusion into the shot. The white rectangle in c represents the area viewed with greater magnification in d.

conservation of morphology imply that the molten In droplets diffuse into the Ni powders rather than leaching away the Ni.

Further support for this hypothesis comes from investigations in the Co−Sn system. Large pieces of Co shot (~5 mm diameter) were added to a TEG dispersion of molten Sn. After reaction, a shell of α-$CoSn_3$ platelets was observed surrounding smaller Co cores (Figure 8c,d). The compositions of both the platelets and the core remnant were confirmed by powder XRD. Taken together, the size and morphology retention in the Ni−In system and the $CoSn_3$ coating on the surface of a millimeter-scale Co shot suggest that the process is diffusion based rather than occurring through leaching or solvation of the transition metal, as would occur in a traditional metal flux reaction.

Conclusions

By reacting molten metal dispersions with fine transition metal and *p*-block metal powders, it is possible to access a variety of binary intermetallic systems at temperatures below 300 °C. The synthetic approach described here bears many similarities to traditional flux methods, which provide for low-temperature synthesis through the use of molten salts or metals as growth media.[9] Traditional flux routes often yield high-purity, crystalline products and have also resulted in the discovery of new ternary and quaternary phases.[25] Similarly, we found that dispersions of molten metals in hot solvents can react at low temperatures with higher melting metal powders to form intermetallics, although the products are polycrystalline. Use of reactive molten metal dispersions in solution allows for rapid synthesis of the low-temperature phase α-$CoSn_3$, which is typically accessed through a lengthy peritectic reaction or with a large excess of Sn flux.[20] This synthetic method is also a viable means of obtaining crystalline, textured intermetallics, such as $FeSn_2$, and bulk-scale quantities of the superconducting phases Bi_3Ni, In_2Bi, and In_5Bi_3.

While this method has proven to be general for the synthesis of a large number of intermetallics, it is limited to systems that contain a low-melting metal and is not likely to provide access to other frequently used flux metals (e.g., aluminum, copper, zinc) with melting temperatures above the boiling point of TEG. Additionally, the diffusion-based growth necessitates inclusion of the molten metal into the final intermetallic phases, precluding synthesis of some of the more exotic phases obtainable through nonreactive flux techniques. Despite these limitations, the presented synthetic strategy is a versatile, robust, and simple means for bulk-scale synthesis of several families of intermetallics. Refluxing TEG also provides slightly reducing conditions,[26] which likely minimize formation of oxide impurities. The ease of sample processing eliminates the need for synthesis in evacuated silica ampoules, facilitates rapid synthesis and time-resolved aliquot studies, and helps to circumvent thermodynamic traps associated with high-temperature synthetic techniques. While it does not yield large single crystals and is not as general as traditional flux methods, this alternative approach yields bulk-scale powders and provides for high-throughput, exploratory intermetallic synthesis in an underexplored low-temperature regime.

Acknowledgment. This work was supported by the U.S. Department of Energy (DE-FG02-06ER46333). Partial support was also provided by the Arnold and Mabel Beckman Foundation (Young Investigator Award), DuPont (Young Professor Grant), the Alfred P. Sloan Foundation (Sloan Research Fellowship), and the Camille and Henry Dreyfus Foundation (Camille Dreyfus Teacher-Scholar Award). Electron microscopy was performed at the Electron Microscopy Facility in the Huck Institutes of the Life Sciences at Penn State. The authors thank Dr. Brian Leonard for help with obtaining SQUID data.

CM800245J

(25) (a) Chondroudi, M.; Balasubramanian, M.; Welp, U.; Kwok, W.-K.; Kanatzidis, M. G. *Chem. Mater.* **2007**, *19*, 4769. (b) Latturner, S. E.; Bilc, D.; Ireland, J. R.; Kannewurf, C. R.; Mahanti, S. D.; Kanatzidis, M. G. *J. Solid State Chem.* **2003**, *170*, 48. (c) Millican, J. N.; Macaluso, R. T.; Young, D. P.; Moldovan, M.; Chan, J. Y. *J. Solid State Chem.* **2004**, *177*, 4695.

(26) Fievet, F.; Lagier, J. P.; Blin, B; Beaudoin, B.; Figlarz, M. *Solid State Ionics* **1989**, *32*, 198.